

See discussions, stats, and author profiles for this publication at: <https://www.researchgate.net/publication/231701705>

# The New Branched Multielectrochromic Materials: Enhancing the Electrochromic Performance via Longer Side Alkyl Chain

ARTICLE *in* MACROMOLECULES · OCTOBER 2011

Impact Factor: 5.8 · DOI: 10.1021/ma2013833

---

CITATIONS

19

---

READS

36

4 AUTHORS, INCLUDING:



**Fatma Baycan Koyuncu**

18 PUBLICATIONS 273 CITATIONS

SEE PROFILE



**Sermet Koyuncu**

Çanakkale Onsekiz Mart Üniversitesi

30 PUBLICATIONS 487 CITATIONS

SEE PROFILE

# The New Branched Multielectrochromic Materials: Enhancing the Electrochromic Performance via Longer Side Alkyl Chain

Fatma Baycan Koyuncu,<sup>\*,†,§</sup> Emre Sefer,<sup>†,§</sup> Sermet Koyuncu,<sup>\*,†,§</sup> and Eyup Ozdemir<sup>†,§</sup>

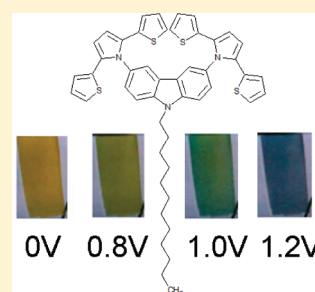
<sup>†</sup>Department of Chemistry, Faculty of Sciences and Arts, Çanakkale Onsekiz Mart University, 17020 Çanakkale, Turkey

<sup>‡</sup>Çan Vocational School, Çanakkale Onsekiz Mart University, 17400 Çanakkale, Turkey

<sup>§</sup>Polymeric Materials Research Laboratory, Çanakkale Onsekiz Mart University, 17020 Çanakkale, Turkey

 Supporting Information

**ABSTRACT:** We describe the synthesis and structure–property relationships of two branched electroactive monomers containing carbazole core, 2,5-di(2-thienyl)-1*H*-pyrrole, differentiated by the length of side alkyl chains (DSNSC-1 and DSNSC-2). Structural identification of initial compounds and products were carried out by using FT-IR and <sup>1</sup>H and <sup>13</sup>C NMR spectroscopy. The electroactive materials DSNSC-1 and DSNSC-2 were directly coated on to ITO glass surface by using electrochemical polymerization process. The results clearly indicate that the length of side alkyl chain has a major impact on optical and electrochemical properties of these polymers. Poly-DSNC-2 with longer side alkyl chain exhibits a high contrast ratio ( $\Delta T\% = 68\%$  at 850 nm), a response time of about 0.8 s, and high coloration efficiency ( $352 \text{ cm}^2 \text{ C}^{-1}$ ) and retained its performance by 97.1% even after 5000 cycles.



## INTRODUCTION

First studies on electrochromic materials started with inorganic semiconductors such as tungsten trioxide ( $\text{WO}_3$ ) and iridium dioxide ( $\text{IrO}_2$ ),<sup>1</sup> and then organic small molecules such as viologens, metallophthalocyanines,<sup>2</sup> and finally conducting polymers, received much attention for electrochromic applications.<sup>3</sup> Construction of conducting polymers that contain multiple redox-active chromophores are important for the preparation of novel polymeric electrochromic materials, which exhibit at least two distinct color states and may give multiple colors, depending on the structure of the material.<sup>4</sup> Besides, conducting polymers have the potential to be used as electrochromic materials because of their structurally controllable HOMO–LUMO band gap by means of easily tuning of colors and also processability, high contrast ability, and fast response time. Furthermore, electrochromic polymers can be switched between their various color states many times without any noticeable decline in performance, so they have been known to possess excellent switching reproducibility.<sup>5</sup> There are a large number of studies about electrochromic polymers with neutral state absorbance that very across the visible region such as high color tunable thiophene based system of the Reynolds group.<sup>6a</sup> Furthermore, these polymers have been reported with neutral state absorbances ranging from the UV for propylenedioxythiophene (ProDOT)–phenylene copolymers<sup>6b</sup> and poly-3,4-(2-ethylhexyloxy)thiophene derivatives<sup>6c</sup> to near-infrared (NIR) for donor–acceptor low-band-gap polymers<sup>6d</sup> such as conjugated system with colors between that range from yellow, orange, red, magenta, blue green, to cyan. Because of these properties, these polymers have been used in many fields such as smart windows, thermal control and thermal emission detectors for spacecraft, camouflage materials in warfare, optical

communications, and biomedical.<sup>3</sup> Also, as the palette of available colors in electrochromic polymers grows, these materials should become more useful for display technology.<sup>6</sup>

Carbazole (Cbz)-based polymers have various advantages such as a strong electron-donating (p-type) chromophore, and also easily functionalized at its (3,6-), (2,7-), or N-positions, and then covalently linked into polymeric systems, both in the main chain as building blocks and in a side chain as subunit.<sup>7</sup> On the other hand, Cbz-based compounds are well-known as a good hole transport and photonic material for optoelectronic devices.<sup>8</sup> Furthermore, poly(3,6-Cbz)s exhibit interesting electrochromic properties because of the conjugation breaks that are present due to the inclusion of a 3,6-linkage. Reynolds et al. suggested that one of the interesting multicolored system is that based upon the 3,6-linked Cbz moiety.<sup>4a–c</sup> Owing to broken conjugation lengths, these polymers generate radical cations which are separated from one another and do not combine. Upon further oxidation at higher potentials, another electron is removed, giving dications. Because of these properties, 3,6-linked Cbz-based electrochromic materials have multiple colors with separate colors present for the neutral, polaronic, and bipolaronic species at various oxidation states.<sup>4a–f,9</sup> On the other hand, recently reported materials, 2,5-di(2-thienyl)-1*H*-pyrrole (SNS) derivatives,<sup>10</sup> have very useful properties for electrochromic applications such as (i) the oxidation potentials of the SNS derivatives is lower (about +0.7 V vs SCE) than that of many of other electroactive materials, (ii) the functionalization of the ter-heteroatom unit by the Paal–Knorr

Received: June 19, 2011

Revised: September 14, 2011

Published: October 13, 2011

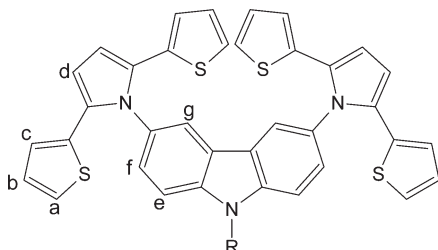
reaction seemed an attractive one step procedure for the introduction of various bridges into the monomer, and (iii) provided that good quality of the films poly-SNS can easily be generated on ITO/glass surface thus high electrochromic performance would be obtained.<sup>11</sup> Furthermore, an electroactive or photoactive moiety is introduced along this SNS backbone to tune the band gap and thus to gain useful properties.<sup>12</sup>

In this article, we report the synthesis of novel derivative of SNS, 3,6-bis(2,5-di-2-thienyl-1*H*-pyrrol-1-yl)-9-ethyl-9*H*-carbazole (DSNSC-1) and 3,6-bis(2,5-di-2-thienyl-1*H*-pyrrol-1-yl)-9-dodecyl-9*H*-carbazole (DSNSC-2), with branched structures and then electrochemically polymerized onto transparent ITO/glass surface to give multielectrochromic polymers. It is determined that the electrochromic performance was strongly improved as a result of prolongation of the side alkyl chain attached to N atom of carbazole molecule. Here we demonstrate that the derivative poly-DSNSC-2 containing dodecyl side alkyl chain exhibits a high contrast ratio ( $\Delta T = 68\%$  at 800 nm), a very short response time (about 0.8 s), a high redox stability, and a high coloration efficiency ( $352 \text{ cm}^2 \text{ C}^{-1}$ ).

## EXPERIMENTAL SECTION

**Materials.** All chemicals were purchased from Aldrich and Fluka and used without further purification. 9*H*-Alkylcarbazole (1),<sup>13</sup> 3,6-dinitro-9*H*-alkylcarbazole (2),<sup>13</sup> 3,6-diamino-9*H*-alkylcarbazole,<sup>13</sup> and 1,4-dithiophene-2-yl-butane-1,4-dione<sup>14</sup> were prepared from previously published procedures.

**Synthesis of 3,6-Bis(2,5-di-2-thienyl-1*H*-pyrrol-1-yl)-9-alkyl-9*H*-carbazole (DSNSCs).** 3,6-Diamino-9*H*-*N*-alkylcarbazole (15 mmol), 1,4-bis(2-thienyl)butane-1,4-dione (45 mmol), and *p*-toluenesulfonic acid (34 mg, 20 mmol) were added into 50 mL of dry toluene. The content of the flask was then refluxed for 72 h under a Dean–Stark trap. The reaction was excused with TLC until initial compounds were consumed. At the end of the reaction, the mixture was cooled and solvent was removed under reduced pressure. The residue was filtered through a short pad of silica gel by eluting with  $\text{CH}_2\text{Cl}_2$  to yield 3,6-bis(2,5-di-2-thienyl-1*H*-pyrrol-1-yl)-9-ethane-9*H*-carbazole (DSNSC-1): 71%; 3,6-bis(2,5-di-2-thienyl-1*H*-pyrrol-1-yl)-9-dodecyl-9*H*-carbazole (DSNSC-2): 64%. FT-IR ( $\text{cm}^{-1}$ ): (C–H aromatic) 3103, 3038; (C–H aliphatic) 2977, 2921, 2862; (C=C phenyl) 1598 1486;  $\delta_{\text{H}}$  (400 MHz;  $\text{CDCl}_3$ ;  $\text{Me}_4\text{Si}$ ): 8.02 (s, 2H, Ar–H<sub>g</sub>); 7.62 (d, 4H, Ar–H<sub>b</sub>); 7.48 (t, 2H, Ar–H<sub>f</sub>); 6.96 (d, 2H, Ar–H<sub>a</sub>); 6.77 (d, 4H, Ar–H<sub>e</sub>); 6.61 (d, 4H, Ar–H<sub>c</sub>); 6.54 (s, 4H, Ar–H<sub>d</sub>); 4.38 (t, 2H, –N–CH<sub>2</sub>–); 1.96–1.21 (C–H aliphatic; for *N*-dodecyl-carb), 0.92 (t, 3H, R–CH<sub>3</sub>, for *N*-dodecyl-carb), 1.45 (t, 3H, R–CH<sub>3</sub>, for *N*-ethyl-carb)  $\delta_{\text{C}}$  (100 MHz;  $\text{CDCl}_3$ ;  $\text{Me}_4\text{Si}$ ): 138.13, 135.8, 134.9, 131.6, 124.1, 121.6, 119.2, 114.5, 110.7, 109.6, 106.2 (aromatic C) 43.18 (N–CH<sub>2</sub>–, 34. 28–21.27 (N–CH<sub>2</sub>(CH<sub>2</sub>)<sub>10</sub>), 14.54 (–CH<sub>3</sub>; for DSNSC-2), 19.38 (CH<sub>3</sub>; for DSNSC-1).



**Electrochemical Polymerizations (Poly-DSNSCs).** Electrochemical polymerization processes were carried out in a dichloromethane solution of  $2.0 \times 10^{-3} \text{ M}$  DSNSC-1 or DSNSC-2 monomer

and 0.1 M TBAPF<sub>6</sub> by repetitive cycling at a scan rate of  $100 \text{ mV s}^{-1}$ . A platinum wire was used as a counter electrode and Ag/AgCl as reference. The polymer was directly coated onto platinum disk ( $0.02 \text{ cm}^2$ ) or ITO ( $8\text{--}12 \Omega$ ,  $0.8 \times 5 \text{ cm}^2$ , active area adjusted to  $1 \text{ cm}^2$ ). After coating of poly-DSNSCs, the ITO-glass surface was cleaned (i.e., dedoped) electrochemically in a monomer free-electrolyte solution in order to remove the residues. Poly-DSNSCs were found to be very slightly soluble in dichloromethane by agitating in an ultrasonic bath. Then these solutions were used for the measurement of their UV–vis absorption measurements.

**Instrumentation.** FT-IR spectra were recorded by a Perkin-Elmer FT-IR Spectrum One by using the ATR system ( $4000\text{--}650 \text{ cm}^{-1}$ ). <sup>1</sup>H and <sup>13</sup>C NMR (Bruker Avance DPX-400) data were recorded at  $25^\circ \text{C}$  by using  $\text{CHCl}_3\text{-d}$  as a solvent and TMS as an internal standard.

The cyclic voltammetry (CV) technique used for electrochemical measurements was performed by Biologic SP-50 electrochemical workstation. These measurements were carried out under an argon atmosphere, and the electrochemical cell includes an Ag/AgCl as reference electrode (RE), Pt wire as counter electrode (CE), and glassy carbon as working electrode (WE) immersed in 0.1 M TBAPF<sub>6</sub> as the supporting electrolyte. HOMO and LUMO energy levels of the polymers were calculated according to the inner reference ferrocene redox couple  $E^\circ(\text{Fc}/\text{Fc}^+) = +0.41 \text{ V}$  (vs Ag/AgCl) in dichloromethane by using the formula  $E_{\text{HOMO}} = -e(E_{\text{ox}} - E_{\text{Fc}}) + (-4.8 \text{ eV})$ .<sup>15</sup> Onset values of oxidation potentials were taken into account while calculating HOMO energy levels. LUMO energy levels were calculated by the addition of the optical band gap to the HOMO level.

UV–vis spectra were recorded by Perkin-Elmer Lambda-35 spectrophotometer. The absorption spectra of monomers and corresponding polymers were recorded in dichloromethane (liquid phase) or on ITO/glass transparent film (solid phase). The optical band gap ( $E_g$ ) of products were calculated from their low-energy absorption edges ( $\lambda_{\text{onset}}$ ) ( $E_g = 1241/\lambda_{\text{onset}}$ ).<sup>16</sup>

Spectroelectrochemical measurements were carried out to consider absorption spectra of these polymer films under applied potential.<sup>17</sup> The spectroelectrochemical cell consists of a quartz cell, an Ag wire (RE), a Pt wire (CE), and an ITO/glass as transparent working electrode (WE). All measurements were carried out in the 0.1 M TBAPF<sub>6</sub> as supporting electrolyte in acetonitrile.

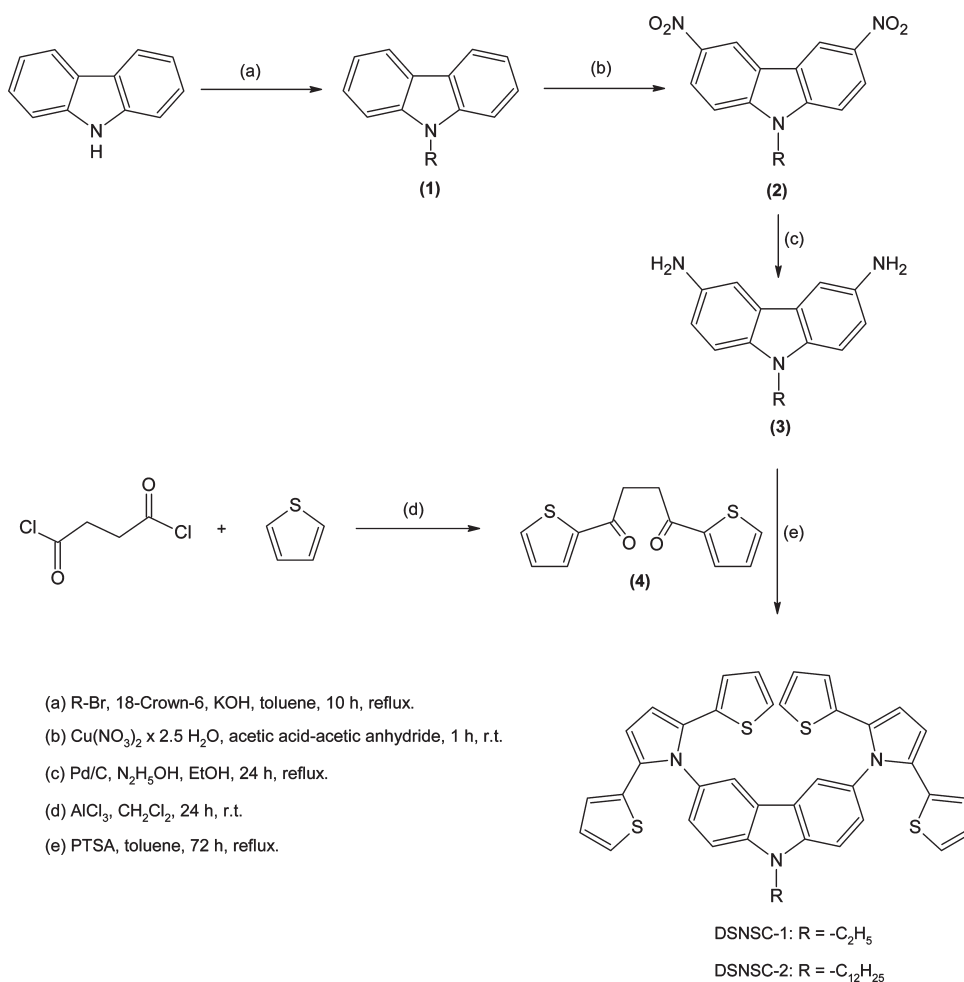
Colorimetry measurements were performed by using Konica Minolta CS-200 chromameter with viewing geometry as recommended by CIE. According to the CIE system, the color is made up of three attributes; luminance (*L*), hue (*a*), and saturation (*b*). These parameters were measured at neutral, intermediate, and fully oxidized state of the electrochromic polymer on the ITO/glass surface.<sup>18</sup>

## RESULTS AND DISCUSSION

**Synthesis and Characterization.** The new electroactive monomers containing Cbz and SNS units with different length of side alkyl chains were synthesized in four steps (Scheme 1). The initial compounds, 9-alkyl-9*H*-carbazole (1), 3,6-dinitro-9-alkyl-9*H*-carbazole (2), and 3,6-diamino-9-alkyl-9*H*-carbazole (3), were synthesized and fully characterized according to the previously reported studies.<sup>13</sup> The final products, DSNSC-1 and -2, were synthesized via Paal–Knorr reaction carried out between 3 and 1,4-dithiophene-2-yl-butane-1,4-dione (4)<sup>14</sup> prepared from thiophene and succinyl chloride in dry toluene in the presence of *p*-toluenesulfonic acid as catalyst.<sup>19</sup> The reaction yields of DSNSC-1 and DSNSC-2 were found to be 71% and 64%, respectively.

After completion of the synthetic works, chemical structures of DSNSCs were elucidated by FT-IR and <sup>1</sup>H NMR. Significant changes were observed between the spectral properties of the

Scheme 1. Synthetic Route to DSNC-1 and DSNC-2



initial compounds and the products. The signals arising from the functional groups of the reactants ( $-\text{NH}_2$  in **3** and  $\text{C}=\text{O}$  bonds in **4**) were disappeared in the FT-IR spectrum of the products of DSNCSs. A characteristic strong peak at  $685 \text{ cm}^{-1}$  was attributed to the formation of pyrrole ring in DSNCSs as a result of the completion of final ring-closure reaction (see Supporting Information). On the other hand, in the  $^1\text{H}$  NMR spectra of DSNCSs, characteristic singlet signal observed at 6.54 ppm is another evidence of this ring-closure reaction. Furthermore, other aromatic signals attributed to thiophene and carbazole moieties were observed as expected. Because of electron-withdrawing effect of nitrogen atom on carbazole, the  $\text{N}-\text{CH}_2$  signal was observed as triplet at higher ppm than other aliphatic protons. Because of the same effect,  $-\text{CH}_3$  end groups of DSNCS-1 and DSNCS-2 were observed at 1.45 and 0.92 ppm as expected (Figure 1), respectively.

**Electrochemical and Optical Properties.** The electrochemical properties of DSNCS monomers and corresponding polymers were investigated by cyclic voltammetry (CV). During CV scan in the anodic regime, DSNCS-1 and DSNCS-2 exhibited semireversible oxidation waves with half-wave potentials ( $E_{\text{m},1/2}^{\text{ox}}$ ) observed at 0.57 and 0.78 V, respectively (Figure 2a,b). DSNCS is a conjugated system which consists of a Cbz as a center and two SNS structures around Cbz center. Therefore, the charges can be delocalized on the conjugated macromolecular structure. If there

are more than one electroactive group and thus expand the conjugation length on an electroactive molecule, two different electron transfer mechanisms, which are intermolecular electron transfer and intramolecular electron transfer, can occur. For the intermolecular electron transfer process, the most important parameter is the distance between the molecules. Because of the shorter alkyl side chain on DSNCS-1, the molecules can approach each other more and the charge interaction between them become higher than that of the DSNCS-2. This effect decreased the oxidation potential pretty much by increasing the ground state energy level (HOMO) of DSNCS-1. Because of all of these reasons, it is clear that oxidation potential of DSNCS-1 is lower than that of DSNCS-2 because of the length of side alkyl chain. Thus, electrochemical polymerization of DSNCS-1 was carried out by repetitive cyclic scans at potentials between 0 and +0.9 V, it exhibited a new redox couple at  $E_{\text{p}1,\text{a}}^{\text{ox}} = 0.55$  and  $E_{\text{p}1,\text{c}}^{\text{ox}} = 0.45$  (Figure 2c). When the second monomer, DSNCS-2, was subjected to the same procedure between 0 and +1.1 V, its new redox couples were observed at  $E_{\text{p}2,\text{a}}^{\text{ox}} = 0.78$  and  $E_{\text{p}2,\text{c}}^{\text{ox}} = 0.66$  (Figure 2d). Because of the extended conjugation as a result of cross-linking occurred between peripheral thiophenes, oxidation potentials of poly-DSNCS-1 and poly-DSNCS-2 occurred as reversible and at lower potentials than the corresponding

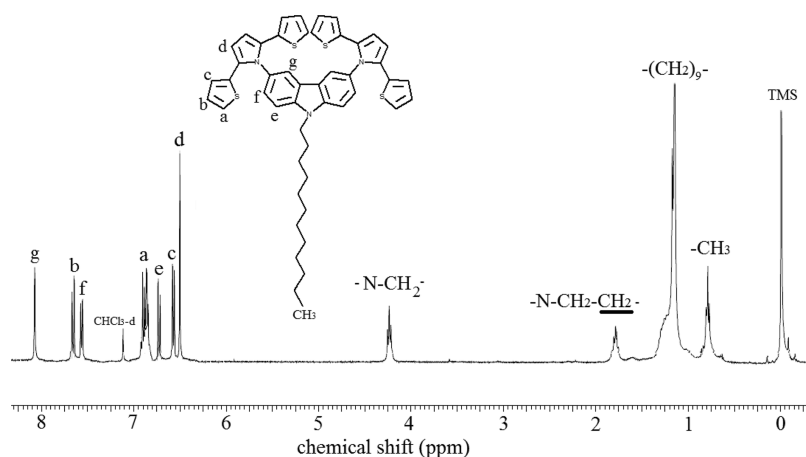


Figure 1.  $^1\text{H}$  NMR spectrum of DSNSC-2.

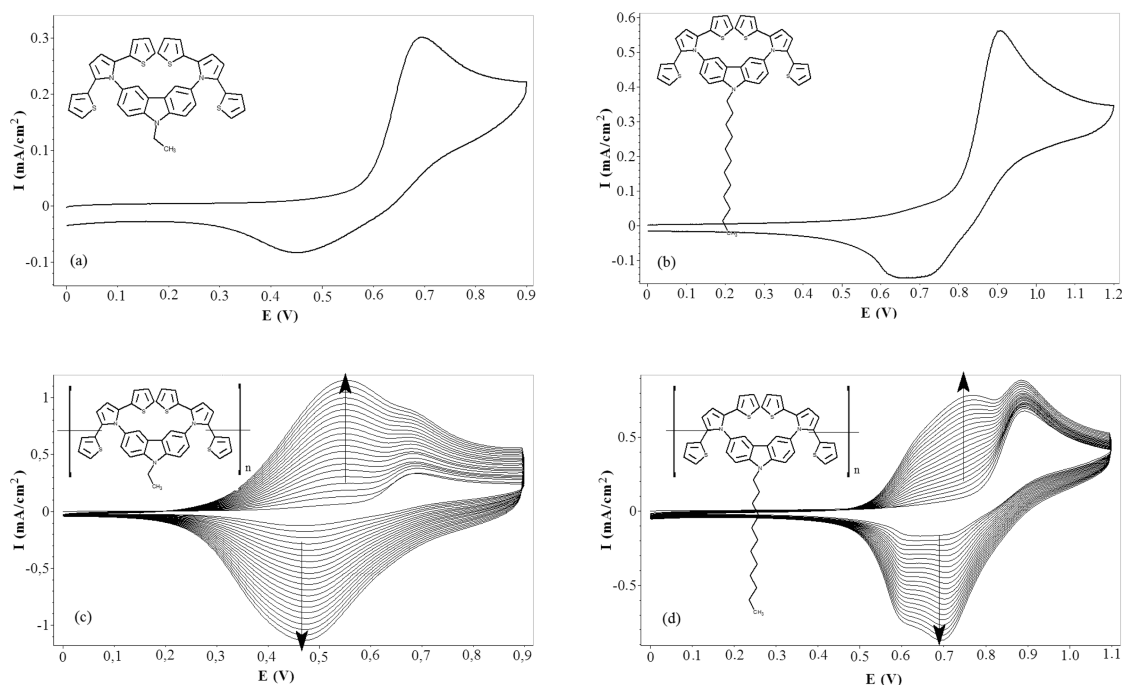


Figure 2. CV of DSNSC-1 (a) and DSNSC-2 (b) and repeated potential scanning of DSNSC-1 (c) and DSNSC-2 (d) with a scan rate of  $100 \text{ mV s}^{-1}$ , vs Ag/AgCl.

monomers. Upon each successive cycle, the intensified oxidation waves clearly indicate the formation of poly-DSNSCs on the surface of working electrode (Figure 2c,d). After coating of poly-DSNSCs onto the substrate, the ITO-glass surface was cleaned (i.e., dedoped) electrochemically in a monomer free-electrolyte solution in order to remove the residues which come from the electrolyte. HOMO energy levels of the monomers and the polymers were calculated according to the onset values of their oxidation potentials, and then their LUMO energy levels were calculated by adding the optical band gap from their HOMO levels (Table 1).

The absorption spectra of DSNSCs and poly-DSNSCs were recorded in the solution phase using dichloromethane (Figure 3). Because of having many photoactive groups in their structures, both of the monomers exhibited multiple absorption bands attributed to  $\pi$ - $\pi^*$  transitions arising from carbazole and SNS

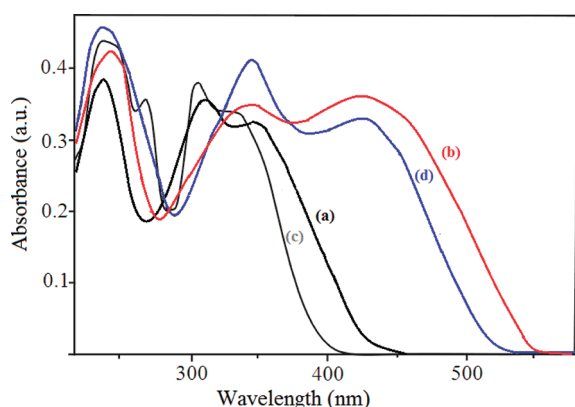
moieties. In addition, the maximum absorption wavelength ( $\lambda_{\text{max}}$ ) showed a blue shift from 351 to 338 nm with the increase in the length of side alkyl chain. Thus, DSNSC-1 has an onset value of 442 nm corresponding to a 48 nm red shift with respect to that of the DSNSC-2. According to these results, the optical band gap values of DSNSC-1 and DSNSC-2 were found to be 2.92 and 3.14 eV, respectively.  $\pi$ - $\pi^*$  conjugation is extended as a result of cross-linking electrochemical polymerization process when going from monomer to the polymer. The absorption bands of poly-DSNSC-1 and poly-DSNSC-2 are broadened and bathochromically shifted with respect to corresponding monomers. As a result of prolongation of side alkyl chain, steric hindrance is promoted, and the molecular structure of the monomer and polymer chains can be separated further from each other. This separation results in significant changes in the optical and electrochemical properties of both monomers and polymers under



**Table 1.** HOMO and LUMO Energy Levels and Optical Band Gap ( $E_g$ ) Values of DSNSCs and Poly-DSNSCs

molecules	oxidation peak potentials (V)	HOMO (eV)	LUMO <sup>a</sup> (eV)	$E_g$ , optical band gap (eV)
DSNSC-1	$E_{m1,a}^{ox} = 0.69$ and $E_{m1,c}^{ox} = 0.45$ semireversible $E_{m1,on}^{ox} = 0.55$	−4.94	−2.11	2.83
DSNSC-2	$E_{m2,a}^{ox} = 0.90$ and $E_{m2,c}^{ox} = 0.67$ semireversible $E_{m2,on}^{ox} = 0.76$	5.15	2.04	3.11
poly-DSNSC-1	$E_{p1,a}^{ox} = 0.55$ and $E_{p1,c}^{ox} = 0.45$ reversible $E_{p1,on}^{ox} = 0.31$	−4.70	−2.44	2.26
poly-DSNSC-2	$E_{p2,a}^{ox} = 0.78$ and $E_{p2,c}^{ox} = 0.66$ reversible $E_{p2,on}^{ox} = 0.52$	−4.91	−2.52	2.39

<sup>a</sup> Calculated by the addition of the optical band gap to the HOMO level.

**Figure 3.** UV-vis absorption spectra of DSNSC-1 (a), poly-DSNSC-1 (b), DSNSC-2 (c), and poly-DSNSC-2 (d) in dichloromethane solution.

investigation. The effect of steric hindrance makes the adjacent electroactive branched structure twisted with respect to each other leading to shorter  $\pi$ -conjugation lengths and lower degree of aggregate formation.<sup>20</sup> Although  $\lambda_{max}$  of poly-DSNSC-1 and poly-DSNSC-2 are the same, the absorption band of poly-DSNSC-1 is more broadened with respect to poly-DSNSC-2. Finally, for poly-DSNSC-1, the onset absorption is observed at 549 nm which corresponds to an energy band gap of 2.26 eV. Besides, the poly-DSNSC-2 has an onset value of 528 nm (equal to a band gap of 2.35 eV) which means a 21 nm red shift with respect to that of the poly-DSNSC-1.

**Spectroelectrochemical Properties.** Owing to spectroelectrochemical measurements, both the electronic structure and optical behavior of poly-DSNSC-1 and poly-DSNSC-2 coated onto ITO/glass surface upon p-doping process can be explained. As each potential is stepped, the absorption in the visible regime begins to decrease, whereas that in the NIR regime increases, indicating the creation of lower energy polaron and bipolaron charge carriers at the expense of the  $\pi$ - $\pi^*$  transition. At the fully oxidized state, the DSNSC polymers have a strong absorption in the NIR that tails into the visible, giving the polymers DSNSC-1 and -2, oily green and dark blue color due to residual red light absorbance, respectively. Reynolds et al. suggested that one of the interesting multicolored system is that based upon the

3,6-linked carbazole moiety.<sup>4a-c</sup> Because of conjugation breaks present due to the inclusion of the 3,6-linked carbazole units, the radical cations are separated from one another and do not combine. Upon further oxidation at higher potentials, another electron is removed, giving dications. The ability of these materials to support two distinct oxidation states leads to multiple color electrochromic effect, with separate colors present for the neutral, polaronic, and bipolaronic species. For poly-DSNSC-1, during the scan from 0 to 0.6 V (Figure 4a), the valence and conduction band ( $\lambda_{max}$ ,  $\pi$ - $\pi^*$  transition) at about 410 nm decreased, and new absorption bands were observed at 770 nm (Figure 4b). At higher potentials (0.6–1.2 V) (Figure 4a), the band at 770 nm gradually intensified and broadened and bathochromically shifted as well (Figure 4b). Furthermore, intensification of broad band at the near-IR region indicates the formation of polarons and bipolarons on poly-DSNSC-1 structure (Figure 4). During the oxidation process, the light brown color of the polymeric film (according to the color parameters of Commission Internationale de l'Eclairage, CIE; luminance  $L$ : 40; hue  $a$ : 15; saturation  $b$ : 37) changed first to brown ( $L$ : 37;  $a$ : 3;  $b$ : 28) and then oily green ( $L$ : 35;  $a$ : 2;  $b$ : 23).

On the other hand, the poly-DSNSC-2 had one maximum absorption band at 418 nm ( $\lambda_{max}$ ,  $\pi$ - $\pi^*$  transition) at the neutral state. Upon oxidation (Figure 5a), the intensity of  $\lambda_{max}$  was simultaneously decreased up to a certain first and second broad bands intensified at about 735 nm (0–0.8 V) and 860 nm (0.8–1.2 V) (Figure 5b) which indicates the formation of polarons and bipolarons on poly-DSNSC-2 film, respectively (Figure 5).<sup>12a</sup> Thus, the NIR region, above 700 nm, was strongly absorbed at fully oxidized state. On the basis of the foregoing results, the light brown color of the film with CIE color parameters ( $L$ : 51;  $a$ : 5;  $b$ : 43) turned into oily green ( $L$ : 46;  $a$ : −11;  $b$ : 36), dark green ( $L$ : 41;  $a$ : −21;  $b$ : 6), and dark blue ( $L$ : 31;  $a$ : −1;  $b$ : −26), respectively (Figure 4b). However, the results of poly-DSNSC-1 compared to that of poly-DSNSC-2 in order to get further support for the effect of prolongation of side alkyl chain. Especially, poly-DSNSC-2 film exhibits a high contrast change in the near-IR region, and it may be one of the most important materials to be used for the near-IR applications.<sup>21</sup>

The double-step chronoamperometry technique was used to monitor the changes in the electro-optical responses during electrochemical switching. Electrochromic parameters of the polymer films were investigated by the changes that occurred in the

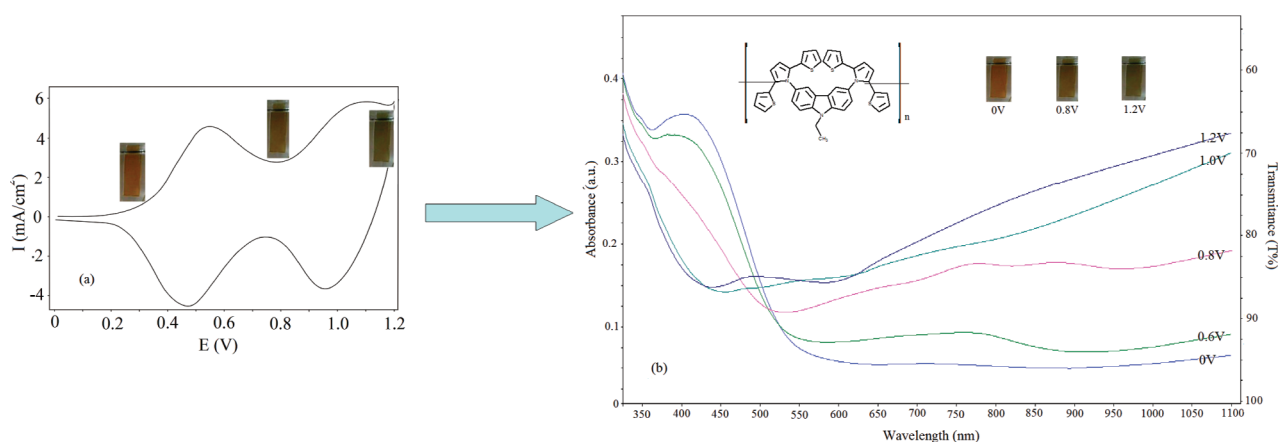


Figure 4. Spectroelectrochemical measurements and color changes of poly-DSNSC-1 film onto the ITO/glass surface.

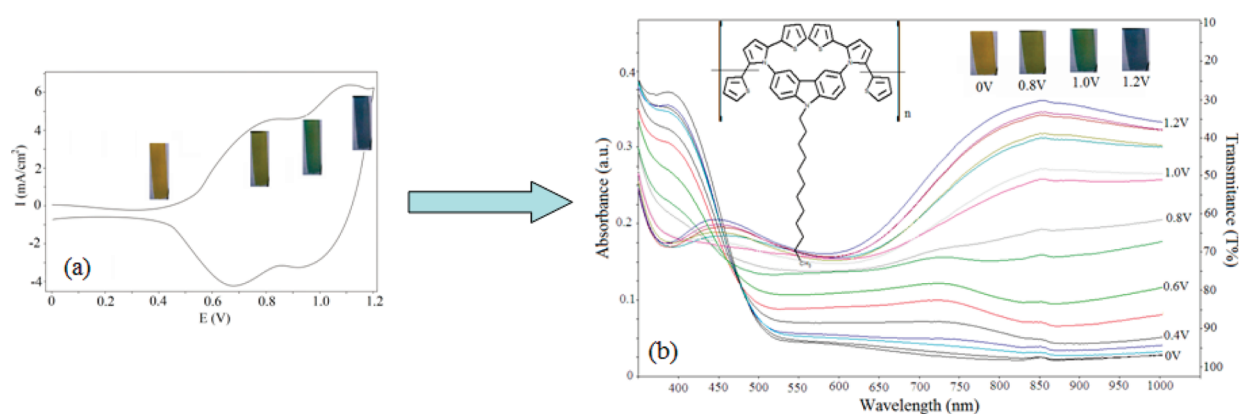


Figure 5. Spectroelectrochemical measurements and color changes of poly-DSNSC-2 film onto ITO/glass surface.

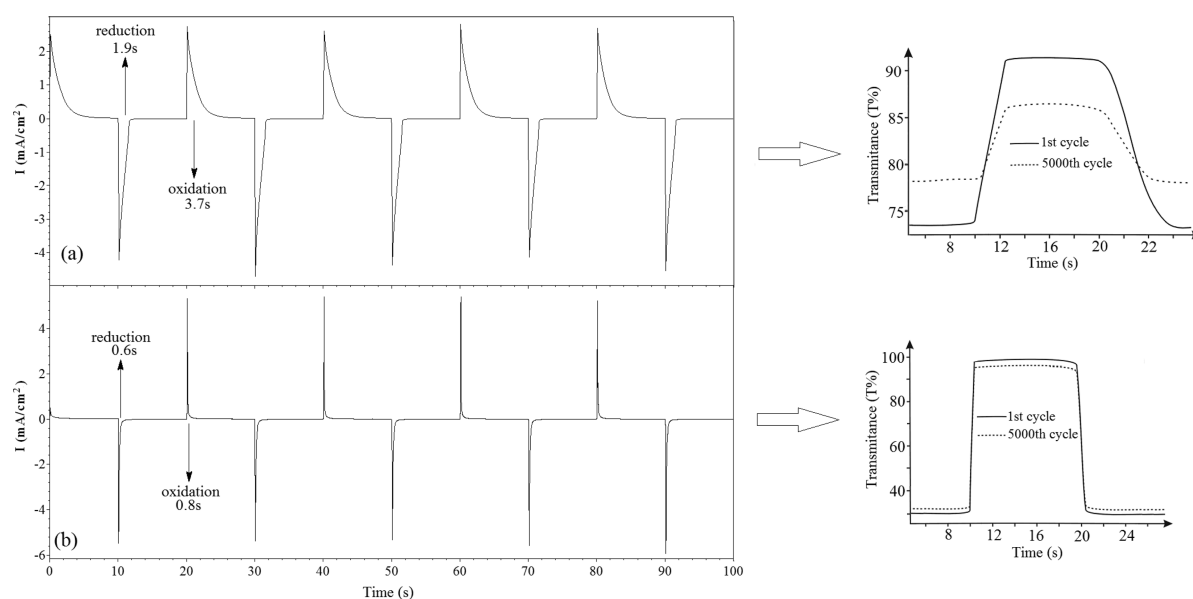


Figure 6. Electrochromic switching, optical absorbance monitored for poly-DSNSC-1 (a) and poly-DSNSC-1 (b) films at 850 nm (0–1.2 V).

transmittance (increments and decrements of the absorption band at 400 and 850 nm with respect to time) while switching the potential stepwisely between neutral and oxidized states with a

residence time of 10 s.<sup>18</sup> The percentage transmittance changes ( $\Delta T\%$ ) of poly-DSNSC-1 between neutral (at 0 V) and oxidized states (at 1.2 V) were found to be 11% for 400 nm and 21% for

Table 2. Electrochromic Parameters for the Poly-DSNSC-1 and Poly-DSNSC-2

molecules	optical contrast change ( $\Delta T\%$ )		response time (s)	optical activity after 5000 cycles (%)	CIE color parameters: luminance ( $L$ ); hue ( $a$ ); saturation ( $b$ )	coloration efficiency ( $\text{cm}^2 \text{C}^{-1}$ )
	400 nm	850 nm				
poly-DSNSC-1	$\Delta T\%$ : 11	$\Delta T\%$ : 21%	oxidation: 3.7	38.2	neutral state: $L$ : 40; $a$ : 25; $b$ : 37	116
	$T_{\text{neut}}$ : 65%	$T_{\text{neut}}$ : 94%	reduction: 1.9		intermediate state: $L$ : 37; $a$ : 3; $b$ : 28	
	$T_{\text{oxi}}$ : 76%	$T_{\text{oxi}}$ : 73%			oxidized state: $L$ : 35; $a$ : 2; $b$ : 23	
poly-DSNSC-2	$\Delta T\%$ : 41%	$\Delta T\%$ : 68%	oxidation: 0.8	97.1	neutral state: $L$ : 51; $a$ : 5; $b$ : 43	352
	$T_{\text{neut}}$ : 28%	$T_{\text{neut}}$ : 98%	reduction: 0.6		intermediate state: (1) $L$ : 46; $a$ : -11; $b$ : 36; (2) $L$ : 41; $a$ : -21; $b$ : 6	
	$T_{\text{oxi}}$ : 69%	$T_{\text{oxi}}$ : 30%			oxidized state: $L$ : 31; $a$ : -1; $b$ : -26	

850 nm (Figure 4b). For poly-DSNSC-2, these values were determined as 41% for 400 nm and 68% for 850 nm (Figure 5b). Besides, the oxidation and reduction response time were measured as 3.7 and 1.9 s for poly-DSNSC-1 (Figure 6a) and 0.8 and 0.6 s for poly-DSNSC-2 (Figure 6b). While optical activity of poly-DSNSC-1 film was only retained by 38.2%, that value for poly-DSNSC-2 was preserved by a factor of 97.1% even after 5000 cycles of operation. By the consideration of all the data, it can be clearly considered that the electrochromic performance of the polymer with dodecyl chain is superior with respect to the one having ethyl. As a result of prolongation of side alkyl chain, the molecular structure of the monomer and polymer chains can be separated further from each other, and in this way, the aggregation effect is diminished. Thus, dopant ions can more freely move in and out of the space between polymer chains of the electrochromic material during redox switching.<sup>9b</sup> These electro-optical results also reveal that have a very strong redox stability and very short response time because it retains its electrochromic activity even after 5000 switching cycles between reduced and oxidized states (Figure 6). Similar electrochemical behaviors were obtained in our previous studies based on SNS-carbazole derivative.<sup>12a,15,21d</sup> Finally, poly-DSNSC-2 can be regarded as a superior material than the previously reported SNS containing analogues because of the above-mentioned electrochemical and electrochromic performance and data.<sup>11,12</sup> Besides, Sankaran and Reynolds indicated that alkyl-substituted polymers of EDOT (PEDOT-C8 and PEDOT-C14) exhibited a higher degree of electrochromic performances when compared to the unsubstituted PEDOT.<sup>22</sup> They reported that the optical contrast ( $T\%$ ) of PEDOT-C14 in the oxidized film was 60% transmissive while the reduced film was less than 5% transmissive ( $\Delta T\% = 55\%$ ).<sup>19</sup> When compared to these reported values of PEDOT-C14, the contrast value of poly-DSNSC-2 is found to be 98% and 30% ( $\Delta T\% = 68\%$ ) in the neutral and oxidized forms, respectively. On the other hand, the optical activity of PEDOT-C14 was conserved by a factor of 60% after 1000 cycles. The electrochromic performance and data of poly-DSNSC-2 make it a better material than various corresponding polymeric electrochromes. Finally, it can be concluded that the enhanced performance of poly-DSNSC-2 has been due to its self-aggregation and barrier effect of longer alkyl chains.

On the other hand, the coloration efficiency (CE) is one of the most important parameters for the electrochromic application.<sup>20</sup> CE was calculated by using  $\text{CE} = \Delta\text{OD}/Q_d$  and  $\Delta\text{OD} = \log(T_{\text{colored}}/T_{\text{bleached}})$ , where  $Q_d$  is the injected/ejected charge between neutral and oxidized states;  $T_{\text{colored}}$  and  $T_{\text{bleached}}$  are the transmittance in the oxidized and neutral states, respectively. Using these equations, while switching the polymer film (coated

onto ITO glass surface with an active area of  $1 \text{ cm}^2$ ) between 0 and 1.2 V, CE of poly-DSNSC-1 and poly-DSNSC-2 was measured as 352 and  $116 \text{ cm}^2 \text{C}^{-1}$  by chronoamperometry, respectively. These results clearly show that the CE value of poly-DSNSC-2 is  $\sim 3$  times greater than that of poly-DSNSC-1. In consequence, this coloration efficiency of poly-DSNSC-2 is one of the highest values in the literature.<sup>11,12,19</sup>

## CONCLUSION

Herein, we report the syntheses of a series of branched electroactive monomers containing Cbz and SNS moieties with different length of side alkyl chains. After completion of the structural characterization, DSNSC-1 and DSNSC-2 were directly polymerized by electrochemical means onto transparent ITO/glass surface to give electrochromic polymer film. Optical and electrochemical properties of DSNSCs and corresponding polymers were greatly influenced by prolongation of the side alkyl chain. Because of self-aggregation and barrier effect, poly-DSNSC-2 having longer alkyl chain exhibits very stable multielectrochromic behavior with a high contrast ratio in the NIR region ( $\Delta T\% = 68\%$  at 850 nm). Because of this property, it can be used as NIR filter for various applications. Compared to all data, it is clearly indicated that the electrochromic performance of poly-DSNSC-2 is superior with respect to poly-DSNSC-1. The various electrochemical and electrochromic data such as reversible redox behavior, low response time, high resistance to over oxidation, low driving voltage, and high coloration efficiency can be absolutely used to indicate that poly-DSNSC-2 would be promising material for the construction and/or the development of electrochromic devices and optical displays.

## ASSOCIATED CONTENT

**S Supporting Information.** FT-IR and  $^1\text{H}$  NMR spectra of initial compounds. This material is available free of charge via the Internet at <http://pubs.acs.org>.

## AUTHOR INFORMATION

### Corresponding Author

\*Fax +90-286-2180533, Tel +90-286-2180018, e-mail fatmabaycan@hotmail.com (F.B.K.); Fax +90-286-4167706, Tel +90-286-4167705, e-mail sermetkoyuncu@hotmail.com (S.K.).

## ACKNOWLEDGMENT

We gratefully acknowledge the support from Çanakkale Onsekiz Mart University Grants Commission (Project No. 2010/60).



## REFERENCES

- (1) (a) Granqvist, C. G. *Electrochim. Acta* **1999**, *44*, 3005–3015. (b) Deuchert, K.; Hunig, S. *Angew. Chem., Int. Ed. Engl.* **1978**, *17*, 875–886.
- (2) Somani, P. R.; Radhakrishnan, S. *Mater. Chem. Phys.* **2003**, *77*, 117–133.
- (3) (a) Monk, P. M. S.; Mortimer, R. J.; Rosseinsky, D. R.; *Electrochromism: Fundamentals and Applications*; VCH: Weinheim, Germany, 1995. (b) Skotheim, T. A.; Reynolds, J. R. *Handbook of Conducting Polymers*, 3rd ed.; CRC Press: Boca Raton, FL, 2007.
- (4) (a) Reddinger, J. L.; Sotzing, G. A.; Reynolds, J. R. *Chem. Commun.* **1996**, 1777–1778. (b) Sotzing, G. A.; Reddinger, J. L.; Katritzky, A. R.; Soloduch, J.; Musgrave, R.; Reynolds, J. R. *Chem. Mater.* **1997**, *9*, 1578–1587. (c) Witker, D.; Reynolds, J. R. *Macromolecules* **2005**, *38*, 7636–7644. (d) Otero, L.; Sereno, L.; Fungo, F.; Liao, Y.-L.; Lin, C.-Y.; Wong, K.-T. *Chem. Mater.* **2006**, *18*, 3495–3502. (e) Natera, J.; Otero, L.; Sereno, L.; Fungo, F.; Wang, N.-S.; Tsai, Y.-M.; Hwu, T.-Y.; Wong, K.-T. *Macromolecules* **2007**, *40*, 4456–4463. (f) Natera, L.; Otero, L.; D'Eramo, F.; Sereno, L.; Fungo, F.; Wang, N.-S.; Tsai, Y.-M.; Wong, K. T. *Macromolecules* **2009**, *42*, 626–635. (g) Rauh, R. D.; Wang, F.; Reynolds, J. R.; Meeker, D. L. *Electrochim. Acta* **2001**, *46*, 2023–2029. (h) Cirpan, A.; Argun, A. A.; Grenier, C. R. G.; Reeves, B. D.; Reynolds, J. R. *J. Mater. Chem.* **2003**, *13*, 2422–2428. (i) Kaya, E.; Balan, A.; Baran, D.; Cirpan, A.; Toppare, L. *Org. Electron.* **2011**, *12*, 202–209.
- (5) (a) Beaujuge, P. M.; Reynolds, J. R. *Chem. Rev.* **2010**, *110*, 268–320. (b) Sonmez, G.; Sonmez, H. B.; Shen, C. K. F.; Jost, R. W.; Rubin, Y.; Wudl, F. *Macromolecules* **2005**, *38*, 669–675. (c) Schwendeman, I.; Hickman, R.; Sonmez, G.; Schottland, P.; Zong, K.; Welsh, D. M.; Reynolds, J. R. *Chem. Mater.* **2002**, *14*, 3118–3122. (d) Durmus, A.; Gunbas, G. E.; Camurlu, P.; Toppare, L. *Chem. Commun.* **2007**, 3246–3248. (e) Liou, G. S.; Hsiao, S. H.; Huang, N. K.; Yang, Y. L. *Macromolecules* **2006**, *39*, 5337–5347. (f) Wang, H.-M.; Hsiao, S. H.; Liou, G. S.; Sun, C. H. *J. Polym. Sci., Part A: Polym. Chem.* **2010**, *48*, 4775–4789. (g) Amb, C. M.; Kerszulis, J. A.; Thompson, E. J.; Dyer, A. L.; Reynolds, J. R. *Polym. Chem.* **2011**, *2*, 812–814. (h) Dyer, A. L.; Craig, M. R.; Babiarz, J. E.; Kiyak, K.; Reynolds, J. R. *Macromolecules* **2010**, *43*, 4460–4467.
- (6) (a) Dyer, A. L.; Thompson, E. J.; Reynolds, J. R. *ACS Appl. Mater. Interfaces* **2011**, *3*, 1787–1795. (b) Amb, C. M.; Dyer, A. L.; Reynolds, J. R. *Chem. Mater.* **2011**, *23*, 397–415.
- (7) (a) Grazulevicius, J. V.; Strohriegel, P.; Pielichowski, J.; Pielichowski, K. *Prog. Polym. Sci.* **2003**, *28*, 1297–1313. (b) Morin, J.-F.; Leclerc, M.; Ades, D.; Siove, A. *Macromol. Rapid Commun.* **2005**, *26*, 761–778. (c) Blouin, N.; Leclerc, M. *Acc. Chem. Res.* **2008**, *41*, 1110–1119. (d) Walkim, S.; Aich, B.-R.; Tao, Y.; Leclerc, M. *Polym. Rev.* **2008**, *48*, 432. (e) Blouin, N.; Michaud, A.; Leclerc, M. *Adv. Mater.* **2007**, *19*, 2295–2300.
- (8) (a) Promarak, V.; Ichikawa, M.; Sudyoadsuk, T.; Saengsuwan, S.; Jungsuttiwong, S.; Keawin, T. *Synth. Met.* **2007**, *157*, 17–22. (b) Ho, M.; Balaganesan, B.; Chu, T.; Chen, T.; Chen, C. H. *Thin Solid Films* **2008**, *517*, 943. (c) Usluer, O.; Demic, S.; Egbe, D. A. M.; Birckner, C.; Tozlu, C.; Pivrikas, A.; Ramil, A. M.; Sariciftci, N. S. *Adv. Funct. Mater.* **2010**, *23*, 4152–4161.
- (9) (a) Koyuncu, S.; Gultekin, B.; Zafer, C.; Bilgili, H.; Can, M.; Demic, S.; Kaya, I.; Icli, S. *Electrochim. Acta* **2009**, *54*, 5694–5702. (b) Usluer, O.; Koyuncu, S.; Demic, S.; Janssen, R. A. J. *J. Polym. Sci., Part B: Polym. Phys.* **2011**, *49*, 333–341. (c) Baycan Koyuncu, F.; Koyuncu, S.; Ozdemir, E. *Electrochim. Acta* **2010**, *55*, 4935–4941.
- (10) (a) Ferraris, J. P.; Skiles, G. D. *Polymer* **1987**, *28*, 179–182. (b) Ferraris, J. P.; Andus, R. G.; Hrcir, D. J. *Chem. Soc., Chem. Commun.* **1989**, *18*, 1318–1320.
- (11) (a) Just, P. E.; Chane-Ching, K. I.; Lacaze, P. C. *Tetrahedron* **2002**, *58*, 3467–3472. (b) Varis, S.; Ak, M.; Akhmedov, I. M.; Tanyeli, C.; Toppare, L. *J. Electroanal. Chem.* **2007**, *603*, 8–14. (c) Varis, S.; Ak, M.; Tanyeli, I. C.; Akhmedov, M.; Toppare, L. *Solid State Sci.* **2006**, *8*, 1477–1483. (d) Yigitsoy, B.; Varis, S.; Tanyeli, C.; M. Akhmedov, I.; Toppare, L. *Thin Solid Films* **2007**, *515*, 3898–3904.
- (12) (a) Koyuncu, S.; Zafer, C.; Sefer, E.; Baycan Koyuncu, F.; Demic, S.; Kaya, I.; Ozdemir, E.; Icli, S. *Synth. Met.* **2009**, *159*, 2013–2021. (b) Cihaner, A.; Algi, F. *Electrochim. Acta* **2008**, *53*, 2574–2579. (c) Cihaner, A.; Algi, F. *Electrochim. Acta* **2008**, *54*, 665–670. (d) Cihaner, A.; Algi, F. *Electrochim. Acta* **2008**, *54*, 786–792. (e) Yavuz, A.; Bezgin, B.; Aras, L.; Onal, A. M. *J. Electroanal. Chem.* **2010**, *639*, 116.
- (13) Koyuncu, S.; Kaya, I.; Baycan Koyuncu, F.; Ozdemir, E. *Synth. Met.* **2009**, *159*, 1034–1042.
- (14) Schweiger, L. F.; Ryder, K. S.; Morris, D. G.; Glidle, A.; Cooper, J. M. *J. Mater. Chem.* **2000**, *10*, 107–114.
- (15) Yu, G.; Yang, Y.; Cao, Y.; Pei, Q.; Zhang, C.; Heeger, A. J. *Chem. Phys. Lett.* **1996**, *259*, 465–468.
- (16) Patil, A. O.; Heeger, A. J.; Wudl, F. *Chem. Rev.* **1988**, *88*, 183–200.
- (17) (a) Wudl, F.; Meng, F. H.; Sonmez, G. *Chem. Mater.* **2004**, *16*, 574–580. (b) Kaim, W.; Fiedler, J. *Chem. Soc. Rev.* **2009**, *38*, 3373–3382. (c) Bange, K.; Gambke, T. *Adv. Mater.* **1990**, *2*, 10–16.
- (18) Thompson, B. C.; Schottland, P.; Sonmez, G.; Reynolds, J. R. *Synth. Met.* **2001**, *119*, 333–334.
- (19) Koyuncu, S.; Usluer, O.; Can, M.; Demic, S.; Icli, S.; Sariciftci, N. S. *J. Mater. Chem.* **2011**, *21*, 2684–2693.
- (20) (a) McCulloch, R. D.; Lowe, R. D.; Jayaraman, M.; Anderson, D. L. *J. Org. Chem.* **1993**, *58*, 904–912. (b) McCullough, R. D.; Tristam-Nagle, S.; Williams, S. P. *J. Am. Chem. Soc.* **1993**, *115*, 4910–4911. (c) Roncali, J. *Chem. Rev.* **1997**, *97*, 173–206.
- (21) (a) Zheng, Y.; Zheng, J.; Dou, L.; Qiao, W.; Wan, X. *J. Mater. Chem.* **2009**, *19*, 8470–8477. (b) Bergeron, B. V.; White, K. C.; Boehme, J. L.; Gelb, A. H.; Joshi, P. B. *J. Phys. Chem. C* **2008**, *112*, 832–838. (c) He, Y.; Zhao, Y. *J. Phys. Chem. C* **2008**, *112*, 61–68. (c) Liou, G. S.; Yen, H. J.; Chiang, M. C. *J. Polym. Sci., Part A: Polym. Chem.* **2009**, *47*, 5378–5385. (d) Sefer, E.; Baycan Koyuncu, F.; Oguzhan, E.; Koyuncu, S. *J. Polym. Sci., Part A: Polym. Chem.* **2010**, *48*, 4419–4427. (e) Yen, H. J.; Lin, H. Y.; Liou, G. S. *Chem. Mater.* **2011**, *23*, 1874–1882. (f) Holt, A. L.; Wehner, J. G. A.; Hamm, A.; Morse, D. E. *Macromol. Chem. Phys.* **2010**, *211*, 1701–1707. (g) Yen, H. Y.; Liou, G. S. *Chem. Mater.* **2009**, *21*, 4062–4070.
- (22) Sankaran, B.; Reynolds, J. R. *Macromolecules* **1997**, *30*, 2582–2588.